Class 1A PI3K regulates vessel integrity during development and tumorigenesis

Tina L. Yuan*†, Hak Soo Choi‡, Aya Matsui‡, Cyril Benes†, Eugene Lifshits§, Ji Luo¶, John V. Frangioni‡, and Lewis C. Cantley*†‖

Departments of *Systems Biology and ¶Genetics, Harvard Medical School, Boston, MA 02115; Divisions of †Signal Transduction and ‡Hematology/Oncology, Beth Israel Deaconess Medical Center, Boston, MA 02115; and §Massachusetts General Hospital Cancer Center, Charlestown, MA 02129

Contributed by Lewis C. Cantley, April 29, 2008 (sent for review April 17, 2008)

PI3K is important in the regulation of growth, proliferation, and survival of tumor cells. We show that class 1A PI3K is also critical in the tumor microenvironment by regulating the integrity of the tumor vasculature. Using Tie2Cre-mediated deletion of the PI3K regulatory subunits (p85α, p55α, p50α, and p85β), we generated mice with endothelial cell-specific loss of class 1A PI3K. Complete loss of all subunits caused acute embryonic lethality at E11.5 due to hemorrhaging, whereas retention of a single p85α allele yielded viable mice that survived to adulthood. These heterozygous mice exhibited no vascular defects until challenged with a pathological insult, such as tumor cells or high levels of VEGF. Under these pathological conditions, heterozygous mice exhibited localized vascular abnormalities, including vessel leakage and the inability to maintain large vessels, which caused a deceleration of tumorigenesis. Furthermore, we show that a PI3K inhibitor can mimic the effects of class 1A PI3K loss, which suggests that targeting class 1A PI3K may be a promising therapy for blocking tumor angiogenesis.

angiogenesis | neovasculature | endothelium

Activating mutations in *PIK3CA*, the gene encoding the p110α catalytic subunit of PI3K, were recently identified as mechanisms of inducing oncogenic PI3K signaling (1). These mutations join *PIK3CA* amplification, PTEN loss, and AKT mutations in a broad class of genomic aberrations that promote tumorigenesis through up-regulation of the PI3K/AKT pathway (reviewed in refs. 2, 3). Somatic missense mutations in *PIK3CA* are the drivers of over 25% of breast and colorectal carcinomas, where they confer constitutive kinase activity through release from inhibitory interactions with its binding partner, p85, and other yet unknown mechanisms (4, 5). This has been shown to lead to growth factor independence, elevated AKT activity, and transforming potential (6, 7). p110α has therefore become an attractive target for therapeutic intervention, with numerous isoform-specific inhibitors of the enzyme in development for the ablation of cancer cells (2, 8, 9).

We investigate the possibility that an additional benefit to the development of p110α inhibitors is the ability to treat cancer through perturbation of the tumor vasculature. As tumors grow larger, it is essential that *de novo* blood vessel formation occurs to maintain oxygen and nutrient exchange between the tumor periphery and the hypoxic core (10). These vessels are also used by metastatic cells, which intravasate into the lumen and are carried to distant sites for secondary site engraftment (11). Blood vessel formation is regulated by vascular growth factors that are secreted by the tumor and its microenvironment. The primary recipient of these signals is the endothelial cell, which coordinates these signals through activation of growth factor receptors, including VEGFR1–3, TIE-1/2, FGFR1–2, PDGFR-β, and ERBB1–4. Signaling through these receptors regulates endothelial cell proliferation and survival, angiogenic sprouting, and vessel growth, maturation, and permeability (12). Importantly, PI3K is activated downstream of each of these receptors and may be a master regulator of angiogenic signaling in the endothelium. Inhibitors of PI3K may thus act as anti-angiogenic compounds by compromising the integrity of the tumor vasculature and decreasing the likelihood of metastasis.

Class 1A PI3Ks are heterodimers consisting of a regulatory subunit (p85α, p55α, p50α, p85β, p55γ) and a catalytic subunit (p110α, p110β, p110δ) and are activated downstream of receptor tyrosine kinases (13). Many inhibitors are being generated against class 1A due to the frequency of p110α mutations and due to the activation of class 1A PI3K downstream of amplified or mutated receptor tyrosine kinases, such as the ERBB family and c-Met (14, 15). In this study, we characterize the role of class 1A PI3Ks in tumor angiogenesis to evaluate the potential of using PI3K inhibitors as anti-angiogenic therapies. We generate mice with endothelial cell-specific loss of class 1A PI3K and show this class of PI3Ks is critical to the maintenance of vessel integrity. Recently, downstream effectors of the PI3K pathway such as AKT, FOXO1, and the lipid phosphatase PTEN, have been implicated in pathological angiogenesis (16–19). Additionally, the mTOR inhibitor Rapamycin has been shown to decrease microvessel density in xenograft and *in vitro* models (17, 20–22). These data support the use of PI3K pathway inhibitors as anti-angiogenic therapy. Class 1A PI3K inhibitors may have the advantage of avoiding potential metabolic toxicities of AKT inhibitors and of robustly disrupting the tumor vasculature by inhibiting mTOR and other key downstream effectors. Our results reveal that in addition to targeting cancer cells, PI3K inhibitors may have the additional benefit of acting as anti-angiogenic agents.

Results

Generation of Endothelial Cell-Specific Class 1A PI3K-Deficient Mice. To deplete the endothelium of class 1A PI3K activity, mice with germline deletion of *pik3r2* (23) were crossed to mice bearing floxed *pik3r1* alleles (24). These mice were crossed to Tie2Cre transgenic mice, which express Cre recombinase in endothelial cells, and the ROSA26-EGFP reporter strain to verify tissue-specific Cre expression (25, 26). The resultant mice are deficient in expression of the major class 1A PI3K regulatory subunits, p85α, p55α, p50α, and p85β, in endothelial cells. Cre-mediated excision of *pik3r1* in endothelial cells results in instability and degradation of the p110 catalytic subunit (27), thereby ablating class 1A PI3K activity and decreasing overall levels of pAKT and pS6K (Fig. 1).

Author contributions: T.L.Y., C.B., J.L., and L.C.C. designed research; T.L.Y. and E.L. performed research; H.S.C., A.M., and J.V.F. contributed new reagents/analytic tools; T.L.Y., C.B., and L.C.C. analyzed data; and T.L.Y. wrote the paper.

The authors declare no conflict of interest.

Freely available online through the PNAS open access option.

‖To whom correspondence should be sent at: 77 Avenue Louis Pasteur, NRB 1030, Boston, MA 02115. E-mail: lewis_cantley@hms.harvard.edu.

This article contains supporting information online at www.pnas.org/cgi/content/full/0804123105/DCSupplemental.

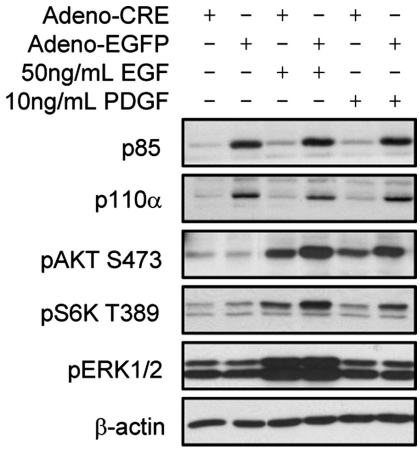

Fig. 1. Loss of p85α and p85β in primary endothelial cells results in decreased PI3K signaling. Primary endothelial cells from p85αflox/flox; p85$\beta-/-$ adult mouse lungs were infected with adeno-CRE or adeno-EGFP virus. Western blot analysis demonstrates that loss of p85 regulatory subunits results in decreased p110α levels and pAKT and pS6K signaling induced by EGF and PDGF.

Class 1A PI3K Loss in the Endothelium Results in Embryonic Lethality due to Hemorrhaging. Complete loss of both p85α and p85β in p85αfl/fl; p85$\beta-/-$; Tie2-Cre+ mice (hereafter referred to as DKO) resulted in embryonic lethality at E11.5. At days E9.5–10.5, DKO embryos were indistinguishable from wild-type and p85β null embryos. Histological analysis revealed well-vascularized yolk sacs and placentas and no developmental abnormalities, suggesting that class 1A PI3K is dispensable for early vasculogenesis including patterning and remodeling (data not shown). The onset of death was observed abruptly at E11.5, concomitant with bleeding and other vascular defects (Fig. 2*A*). Histological analysis of DKO embryos revealed severe vessel dilation and red blood cell congestion (Fig. 2*B*). We also detected breaching of vessel walls (Fig. 2*C*) and widespread hemorrhaging (Fig. 2*D*). These data suggest that class 1A PI3K regulates vessel integrity, which is important in maintaining intact vessel walls and adapting appropriate vascular tone and elasticity. The absence of developmental or other vascular defects in the DKO embryo support a vessel integrity defect as the primary cause of death in these embryos.

Class 1A PI3K-Deficiency in the Endothelium Results in Vascular Leakage. Mice retaining one allele of p85α (p85αfl/+; p85$\beta-/-$; Tie2-Cre+, hereafter referred to as heterozygotes) develop normally to adulthood. To identify defects in the vasculature of these mice, we performed Matrigel plug assays. S.c. implantation of Matrigel with syngeneic B16-F1 melanoma cells elicited a robust angiogenic response under the skin and allowed us to analyze the formation and function of the neovasculature. After 7 and 10 days we visualized the vascular network by retroorbital injection of a near infrared (NIR) dye-conjugated PEG compound (5kD). There was no significant difference in the extent of the vascular network of wild-type and heterozygous mice, as measured by the number of branched vessels (data not shown). This suggests that class 1A PI3K deficiency does not affect vessel sprouting in response to growth factor stimulation. However, there was significant dye extravasation in the heterozygous mutant mice compared with wild-type mice (Fig. 3*A*). We measured intra- and extravascular dye content, and calculated vessel permeability as the ratio of dye outside to dye inside of vessels (values >1.0 indicate leakage). Wild-type vessels maintained permeability ratios significantly under 1.0 (average value = 0.79) following dye injection, while heterozygous mutant vessels quickly surpassed 1.0 (average value = 1.08) [Fig. 3*B* and supporting information (SI) Fig. S1]. After 5 min, wild-type permeability values begin to approach 1.0, indicating dilution of the dye into circulation and slow dye extrusion as expected for small molecules of 5kD. Heterozygous mutant vessels at 5 min maintained steady values of 1.1, indicating that most of the dye was leaked in the first 30–60 seconds (Fig. 3*B*). These data demonstrate that class 1A PI3K-deficiency causes neovasculature leakage.

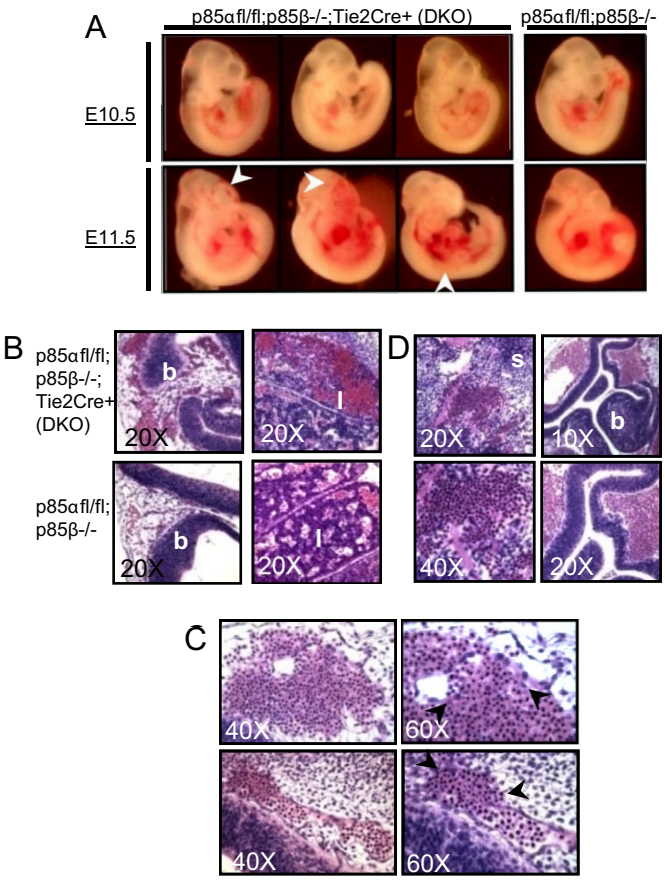

Fig. 2. Class 1A PI3K loss is embryonic lethal at E11.5. (*A*) DKO embryos are indistinguishable from p85$\beta-/-$ littermates at E10.5 and exhibit no developmental delays or vascular abnormalities. At E11.5, DKO embryos exhibit enlarged vessels, microaneurysms, and bleeding (*arrows*) and are often found dead. (*B*) Vessel dilation appears often in the brain (b) and liver (l). The vessels are characterized by large lumens and severe red blood cell congestion. (*C*) Congested vessels in DKO embryos breach under increased pressure. Arrowheads encompass the breach in the vessel wall. (*D*) Breaching of large vessels leads to widespread hemorrhage, shown at the intersomitic region (s) and cortex of the brain (b) of DKO embryos.

Tumor Growth Is Delayed and Decelerated in Heterozygous Mutant Mice. To investigate the effects of endothelial class 1A PI3K deficiency on tumor growth, we s.c. implanted B16-F1 allografts in heterozygous mutant mice and monitored tumor growth daily for 28 days. Wild-type mice developed large tumors (>600 mm^3) as early as day 10, and 79% of mice developed large tumors by day 28 (Fig. 4*A*). These mice also grew tumors nearly synchronously with 47% of mice developing large tumors between the narrow window of day 14–16. Conversely, heterozygous mutant mice were delayed in developing large tumors with the earliest large tumor emerging at day 16. By day 28, only 48% of heterozygous mice developed large tumors. The delay in the formation of large tumors may be explained by the difference in tumor growth rate between wild-type and heterozygous mice. The rate of tumor growth in wild-type mice was generally rapid, reaching exponential growth by day 8, whereas heterozygous

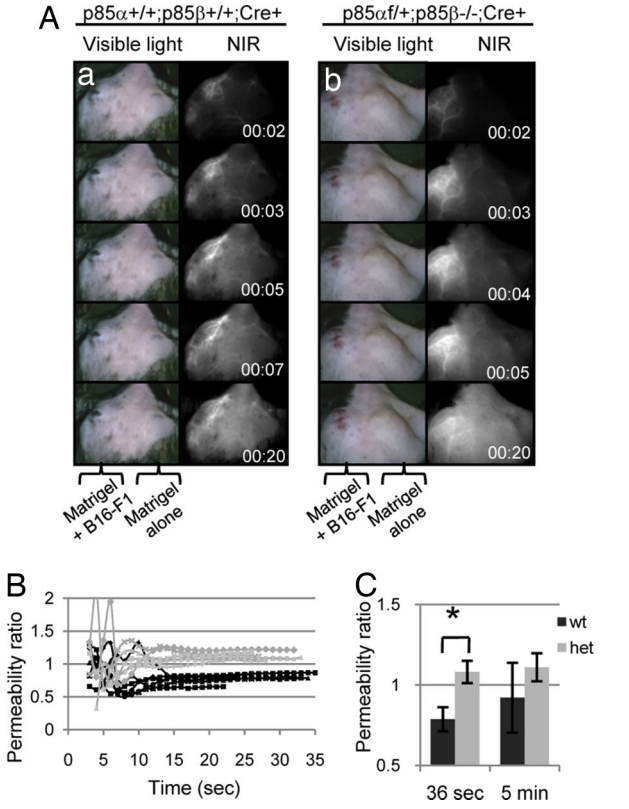

Fig. 3. Heterozygous mice have increased neovasculature permeability. (*A*) Matrigel alone (right flank) or Matrigel containing B16-F1 tumor cells (left flank) was implanted under the skin of wild-type mice and heterozygous mice. Angiogenesis into the region of the Matrigel plug was evaluated by i.v. injection of a NIR dye (see *Materials and Methods*) at 7 or 10 days following implantation. There was no difference between 7 or 10 days of implantation, and both data sets were pooled into one. (*a*) Wild-type and (*b*) heterozygous mice both have a robust angiogenic response, as seen by the abundant vessel growth and branching in the left flank. However, extensive leakage from the neovasculature of the heterozygous mice was observed, as evidenced by the presence of NIR dye in extravascular regions within 4 seconds after i.v. injection. By contrast, the NIR dye remains within the vessels of the wild-type mouse after 20 seconds. (*B*) Ten seconds postinjection, all heterozygous mice exhibited permeability ratios >1.0, indicating leakage (gray lines). All wild-type mice maintained ratios <1.0, indicating dye retention (black lines). (*C*) The average permeability ratio 36 s after dye injection was significantly higher in heterozygotes than in wild types ($P < 0.0001$, Student's *t* test).

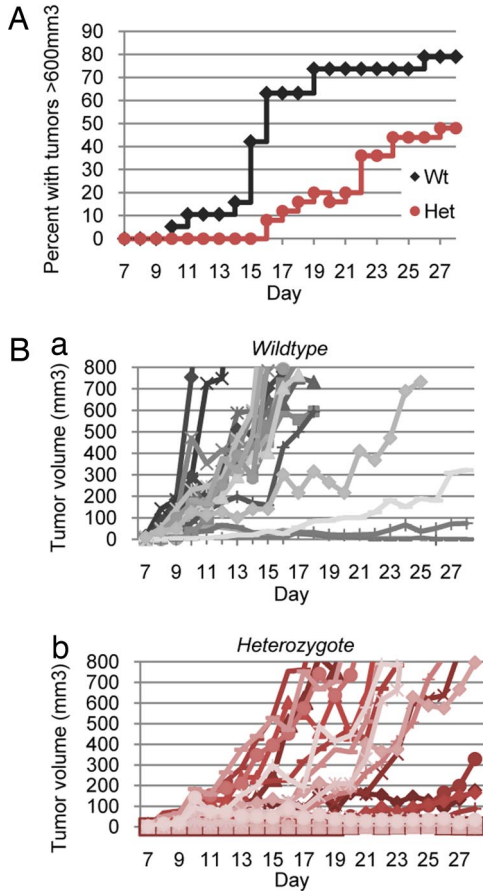

Fig. 4. Class 1A PI3K deficiency causes delayed and decelerated tumorigenesis. (*A*) Percentage of mice with large tumors exceeding 600 mm^3. 8.5×10^5 B16-F1 melanoma cells were injected into the rear flanks of wild-type and heterozygous mice, and tumor volume was measured daily. Wild-type mice grew large tumors as early as 10 days after injection. By day 28, 79% of wild-type mice bore large tumors. By contrast, heterozygous mice were delayed in large tumor formation; tumors were not observed until day 16. By day 28, only 48% of these mice bore large tumors. (*B*) Tumor growth rates varied between wild-type and heterozygous mice. (*a*) The tumor growth rates in wild-type mice were fast and synchronous, with most mice achieving maximal tumor volumes by day 16. (*b*) The tumor growth rates in heterozygous mice were slow and asynchronous, with maximal tumor volumes achieved often only after day 20. Nine of 25 mice (36%) failed to grow tumors or had tumors that regressed.

mutant tumors grew at slower and more variable rates (Fig. 4*B*). Additionally, there was a large subset of heterozygous mutants (9 of 25) that were incapable of forming tumors or grew small tumors that regressed. These data are consistent with the notion that tumor growth was delayed or slowed in the heterozygous mice due to a vascular defect that restricted blood flow to the tumor.

Vessel Size Is Affected by Class 1A PI3K Loss. One possible explanation for the defect in tumor growth in the heterozygous mice is insufficient vessel density to provide oxygen and nutrients for exponential growth. We therefore analyzed large tumors (>600 mm^3) from heterozygous and wild-type mice by staining tumor sections for the endothelial-specific marker, CD31, and measured vessel density. There was no significant difference in vessel density between wild-type and heterozygous mice, regardless of the rate of tumor growth (Fig. S2). These data suggest that the heterozygous mice have a normal angiogenic response to tumorigenic signals including vascular growth factors and hypoxia.

We next examined vessel size by measuring the area of vessel lumens in sections from large tumors (>600 mm^3). Wild-type tumors bore significantly more large (10,000–20,000 surface units, $P < 0.01$) and extra-large (>20,000 surface units, $P < 0.0001$) vessels than heterozygous mice (Fig. 5 *A* and *B*). Wide variation in vessel size distribution was also apparent in wild-type mice, consistent with the haphazard nature of tumor angiogenesis (23), while heterozygous tumors exhibited consistent vessel size distribution (Fig. 5*A*). This suggests that the vasculature in the heterozygous mice had normalized either through the collapse of large abnormal vessels or the inability of small vessels to grow larger. The absence of large vessels may have been compensated for by the sprouting more small vessels, which were slightly more abundant than in wild-type mice (Fig. 5*B*).

To understand the absence of large vessels in the heterozygotes, we stained wild-type and heterozygous vessels for αSMA and cleaved caspase-3. Large heterozygous vessels showed discontinuous staining in 28% of vessels analyzed compared to 17% of wild-type vessels (Fig. 5*C* and data not shown), while small vessels for both wild-type and heterozygous mice stained evenly

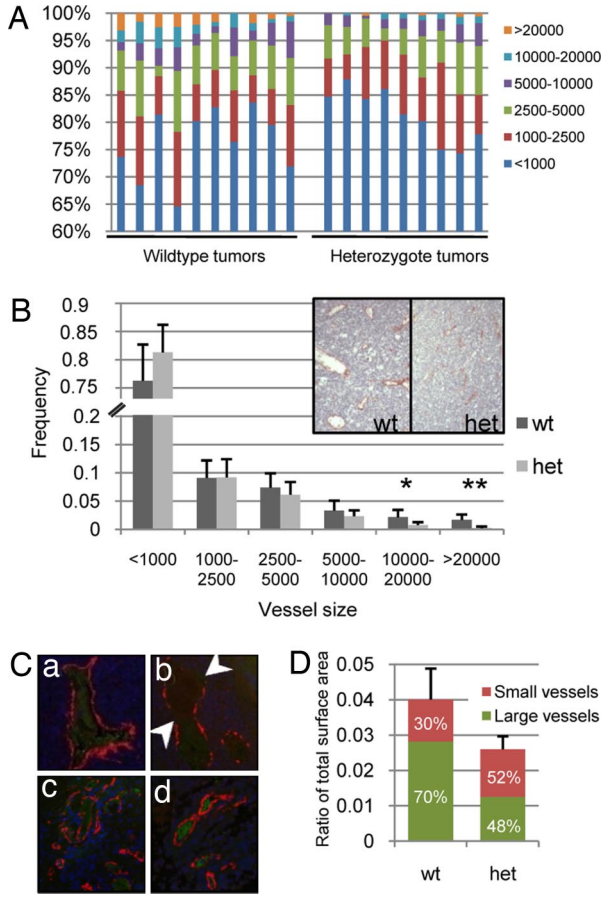

Fig. 5. Heterozygotes are defective in sustaining large vessels. (*A*) Vessel size distribution varied between wild-type and heterozygous mouse tumors. Tumors in wild-type mice bore more large vessels than tumors in heterozygous mice, and exhibited more variation in vessel size distribution. (*B*) Wild-type mice exhibited significantly more large (10,000–20,000) and extra large (>20,000) vessels than heterozygotes ($P < 0.01$ and $P < 0.0001$, respectively). *Inset* shows a representative tumor section from a wild-type and heterozygous mouse, stained for CD31. (*C*) Tumor sections were stained for αSMA (red), cleaved caspase-3 (green), and DAPI (blue). (*a* and *b*) Compared to wild-type mice (*a*), tumors from heterozygous mice (*b* arrows) exhibited more large vessels with discontinuous αSMA staining, indicating a loss of pericytes. (*c* and *d*) However, small vessels of both wild-type (*c*) and heterozygous (*d*) mice were well-encompassed by a continuous layer of αSMA-positive cells. There was no cleaved caspase-3 staining in endothelial cells or pericytes. Red blood cells exhibited slight background staining. (*D*) The absence of large vessels caused a significant decrease in overall luminal area. We show that wild-type and heterozygous tumors are composed of 4.0% and 2.6% vascular space, respectively ($P < 0.0005$; Student's *t* test). Additionally, large vessels account for 70% of the vascular space in wild-type tumors, compared with only 48% in heterozygous tumors. This indicates that wild-type tumors rely heavily on large vessels for their rapid growth.

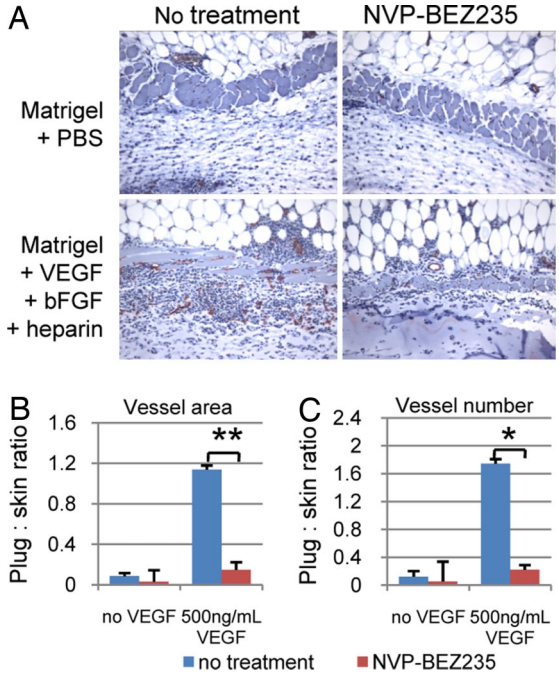

Fig. 6. NVP-BEZ235 treatment affects angiogenesis induced by high concentrations of VEGF. Mice were treated or not treated with 40 mg/kg NVP-BEZ235 and Matrigel plugs infused with PBS or 500 ng/ml VEGF + 600 ng/ml bFGF + 1 μg heparin were implanted in each mouse. After 10 days, the plugs were excised and stained for CD31. Vascularization was measured by comparing the CD31-positive structures in the skin to those in the plug. Induction of angiogenesis would reflect sprouting of new vessels in the plug from extant vessels in the skin. (*A*) Sections containing skin (*Top*) and Matrigel (*Bottom*) were stained for CD31 and counterstained with hematoxylin. (*B*) NVP-BEZ235 significantly reduced the vessel luminal area induced by 500 ng/ml VEGF ($P < 0.0001$; Student's *t* test). (*C*) NVP-BEZ235 also significantly reduced vessel sprouting that was induced by 500 ng/ml VEGF ($P < 0.005$; Student's *t* test).

for αSMA. There was no significant cleaved caspase-3 staining in any of the vessels analyzed. This suggests that endothelial class 1A PI3K deficiency does not affect the recruitment of pericytes/smooth muscle cells to small vessels or the apoptosis of endothelial cells; however, the loss of pericytes/smooth muscle cells in large vessels may affect vessel collapse or failure of small vessels to grow large.

We calculated the contribution of vessel luminal space to the total surface area of the tumor section. Wild-type and heterozygous tumors were composed of 4.0% and 2.6% vessel luminal space, respectively ($P = 0.0005$, Fig. 5*D*). This suggests that the ultimate consequence of class 1A PI3K deficiency in the endothelium is substantial loss of blood flow to the tumor.

Inhibition of PI3K Activity Inhibits Vascularization in Response to High Levels of VEGF. We next investigated the potential efficacy of PI3K inhibitors as anti-angiogenic therapy. We implanted wild-type mice with Matrigel plugs impregnated with PBS or 500 ng/ml VEGF + 600 ng/ml bFGF + 1 μg/ml heparin. The mice were treated or not treated with 40 mg/kg of the pan-PI3K/mTOR inhibitor, NVP-BEZ235, followed by plug excision 10 days postimplantation. The plugs and adjacent skin tissue were analyzed for vessel growth by CD31 staining, and angiogenic response was measured as the ratio of the number and surface area of newly formed vessels within the plug to extant vessels in the skin (Fig. 6*A*). NVP-BEZ235 treatment significantly decreased vessel number and luminal space under conditions of high VEGF concentrations (Fig. 6*B*). These data suggest that NVP-BEZ235 will be effective at inhibiting angiogenesis induced by tumor cells that secrete high levels of VEGF.

Discussion

The results presented in this manuscript indicate that class 1A PI3K plays a critical role in vascular integrity during development as well as during tumor neovascularization. In the endothelium, Tie2 is expressed at E7.5–8.0, and mature endothelial cells emerge around E8.5 to line the vessels of the primitive circulatory system (28). By E9.5, endothelial cells are fully differentiated. DKO embryos develop normally through E10.5, indicating that class 1A PI3K activity in the endothelium is not necessary for endothelial cell differentiation or the formation of the primitive vascular network. The abrupt death of these embryos at E11.5 is concomitant with the maturation of the

endocardium, initiation of discrete pulsatile heartbeats, and increased blood flow velocity (29). We hypothesize that increased hemodynamic stress causes vascular rupture due to loss of vessel integrity. Interestingly, while the DKO exhibit no developmental defects, deletion or activation of downstream effectors of the PI3K pathway results in widespread developmental and structural defects. The defect in vascular integrity appears to be the major reason that germline deletion of class 1A PI3K genes results in embryonic lethality. The p85$\alpha-/-$; p85$\beta-/-$ embryos, and the p110$\alpha-/-$ embryos also exhibit loss of vascular integrity and die at essentially the same stage of development as the endothelial cell-specific knockouts (30). FOXO1 germline deletion results in underdeveloped arteries and early vessel remodeling defects; homozygous PTEN deletion in the endothelium results in abnormal vascular remodeling and bleeding (31, 19). Constitutive AKT activity in the endothelium results in defective vessel patterning in addition to vessel congestion and breaching (32). These and our data support a model in which class 1A PI3K plays an isoform-specific role in maintaining vessel integrity. It is possible that class 1B PI3K regulates early vasculogenesis through activation of AKT, while class 1A is required for vessel maintenance as vessel burden increases. It will be important to understand if class 1A PI3K-specific functions are also dependent on AKT.

The abrupt death and severity of the DKO phenotype made it difficult to characterize the nature of the vascular defect. We were able to isolate an intermediate phenotype by analyzing angiogenesis in adult heterozygous mice. In our Matrigel plug assays, B16 tumor cells provided a constant source of vascular growth factors to trigger a robust angiogenic response in the skin. Our imaging techniques allowed us to visualize vessels in the skin-plug interface. We demonstrate that vessels in the heterozygous mice were leaky compared with wild-type vessels. This suggests that class 1A PI3K-deficiency exacerbates permeabilization caused by chronic exposure to vascular growth factors. Alternatively, the hyperpermeability could be an indicator of a structural defect. In either case, we hypothesized that hyperpermeability of the heterozygotes could lead to complete structural collapse in vessels embedded within tumors due to compression from high interstitial pressure.

S.c. allograft experiments did indeed demonstrate that class 1A PI3K deficiency affects the ability to sustain large vessels within tumors, but has no effect on vessel sprouting. This led us to hypothesize that in heterozygous mice, there is an upper limit to the vascular burden supported by tumor vessels. This threshold is probably defined by the effects of hyperpermeability as well as a discrete structural defect caused by class 1A PI3K loss. Once the threshold is surpassed, the vessels cannot maintain their integrity and fail, inducing growth arrest of tumor cells until a new blood supply can be established. This may explain the slow growth rate and regression of tumors in the heterozygous mice, as well as the asynchrony of tumor growth, which may reflect the sporadic nature of vessel failure.

These experiments were carried out in mice retaining one allele of p85α in the endothelium, which demonstrates that complete ablation of PI3K signaling will not be necessary to elicit an anti-angiogenic effect. In fact, given the role of PI3K and AKT signaling in physiological angiogenesis, metabolism, and normal tissue homeostasis, it would be desirable from a clinical standpoint to administer intermediate doses of PI3K inhibitor for the treatment of cancer. We show that 40 mg/kg of NVP-BEZ235 is effective at inhibiting angiogenesis in response to high or pathological VEGF levels (500 ng/ml). The treated mice exhibited decreased vessel sprouting as well as lower vessel surface area, indicating that this pan-PI3K inhibitor likely decreased overall levels of PI3K activity in the endothelium, not exclusively class 1A PI3K as in our transgenic mice. In concordance with these results, Schnell *et al.* have shown that NVP-BEZ235 treatment affects multiple aspects of tumor angiogenesis including endothelial cell proliferation and vascular permeability to confer marked anti-tumor activity (33). An optimum dosage of this compound will therefore be important to ensure that angiogenesis induced by physiological levels of VEGF will not be affected. These data indicate that NVP-BEZ235 and other PI3K inhibitors will be promising compounds for clinical trials. The utility of these compounds is especially exciting, given that they have the potential to serve as both cytotoxic and anti-angiogenic agents, thereby attacking the tumor on multiple fronts and potentially decreasing the likelihood of metastasis.

Our findings are also interesting in light of the emerging concept of tumor vasculature normalization. Proposed by Rakesh Jain and colleagues, this concept addresses the paradox that destroying the tumor vasculature impedes tumor cell growth but also compromises drug delivery and the efficacy of chemo- and radiation therapy. Jain proposes that certain therapies can restore the balance of pro- and anti-angiogenic signals in the tumor, which leads to normalization of abnormal vessels (reviewed in 34). During this brief window of time, normalization would facilitate drug delivery and alleviate hypoxia, thereby sensitizing cancer cells to treatment. The ability of class 1A PI3K to inhibit the formation of large vessels with limited effects on small vessels complements this emerging paradigm. In this case, normalization is achieved through the absence of large vessels rather than their normalization. The preservation of angiogenic sprouting and small vessel growth within the tumor could then proceed to facilitate drug delivery and alleviate hypoxia.

What remains unclear is the mechanism by which class 1A PI3K regulates vessel integrity. We were unable to detect cleaved caspase-3 in endothelial cells of the heterozygotes or apoptotic nuclear fragments in endothelial cells of DKO embryos. This indicates that canonical survival signals are intact and that the defect may be in another pathway. One possibility is that these enzymes are critical in the maintenance of cell polarity. Endothelial cells are highly polarized, which facilitates the formation of vessels. PI3K plays an intimate role in the polarization of epithelial cells and in chemotaxis in *Dictyostelium* (reviewed in refs. 35, 36). Loss of class 1A PI3K may lead to depolarization or junction disassembly, which could result in weak cell-cell junctions, leakage, and structural failure. Understanding the differences between pathological and physiological angiogenesis, for example, in the rate of growth or integration of growth factors, may also provide clues to the mechanism by which class 1A PI3K regulates vessel integrity.

Materials and Methods

Generation of Mice. p85αflox/flox; p85$\beta-/-$ mice were generated as previously described (24) and crossed with Tie2Cre and ROSA lox-STOP-lox transgenic mice (25, 26). Mice were maintained in a 129/C57B6 background, and all procedures were conducted in accordance with Beth Israel Deaconess Medical Center IACUC guidelines.

Matrigel Plug Assays and *in Vivo* Imaging. Age- and sex-matched heterozygous (p85αflox/+; p85$\beta-/-$; Tie2Cre+) or wild-type (p85αflox/flox; p85β+/+; Tie2Cre- or p85α+/+; p85β+/+; Tie2Cre+) mice were injected s.c. above the rear flanks with 0.3 ml Growth Factor-Reduced Matrigel (BD Biosciences), with and without 1.5×10^6 syngeneic B16-F1 melanoma cells, as described in ref. 37. Ten days after injection, the mice were sedated and hair was removed from the injection sites. Mice were retroorbitally injected with 500 pmol of a near-infrared (NIR) dye-conjugated PEG 5kD (see *SI Text*). The vasculature under the skin was imaged with NIR fluorescence excitation light (725–775 nm) with a 795 nm longpass emission filter. Dye leakage was quantified using custom LabVIEW (National Instruments, Austin, TX) software by comparing NIR intensity of user-defined intravascular and extravascular regions.

Tumor Growth Assay. Age- and sex-matched heterozygous or wild-type mice were injected s.c. above the rear flanks with 8.5×10^5 syngeneic B16-F1 melanoma cells. Tumor dimensions were measured with calipers daily for 28

days or until tumors reached a diameter of 2 cm. Tumor volume was calculated using the formula $0.5233 \times L \times W \times H$. The mice were killed at day 28 or earlier, and tumors were excised.

Matrigel Plug Assay with Inhibitor Treatment. Age- and sex-matched wild-type mice were implanted above the rear flanks with two Matrigel plugs each, impregnated with PBS or 500 ng/ml VEGF-A + 600 ng/ml bFGF + 1 μg/ml heparin. NVP-BEZ235 (Novartis) was orally administered (p.o.) at 40 mg/kg daily beginning two days after injection for five days, followed by two days rest and then one additional day. NVP-BEZ235 was dissolved in 1-methyl-2-pyrrolidone (NMP) and PEG300 for a final concentration of 10% NMP and 90% PEG300. Plugs were excised 10 days postimplantation.

Immunohistochemistry and Immunofluorescence. For CD31 (BD Biosciences) staining, excised tumors and Matrigel plugs were fixed in Zinc/Tris buffer and stained as described in ref. 18. For αSMA (Vector Labs) and cleaved caspase-3 (Cell Signaling) staining, tissues were fixed in formalin. All tissues were paraffin embedded and sectioned for staining. Vessel density in tumors was measured by counting CD31-positive structures in four non-overlapping 20X fields per tumor. Vessel density in Matrigel plugs was measured by comparing CD31-positive structures in the skin with those in the plug in four non-overlapping 20X fields per plug. Vessel size was measured by tracing the circumference of the lumen of individual vessels with the ''Lasso'' tool in Adobe Photoshop. Total pixel units within each CD31-positive region represented the luminal area of a single vessel.

Primary Endothelial Cell Isolation. Endothelial cells were isolated from p85αflox/flox; p85$\beta-/-$ adult mouse lungs using CD31-conjugated Dynabead separation (Invitrogen). See SI for details.

Western Blotting. Immortalized p85αflox/flox; p85$\beta-/-$ endothelial cells were infected with adenovirus (Ad5CMVCre-eGFP or Ad5CMVeGFP, University of Iowa) at an MOI of 70. Forty-eight hours later, 2×10^5 cells were seeded on gelatin coated 6-well plates and starved overnight in EBM-2/1% inactivated FBS/ penicillin/streptomycin. Cells were stimulated with 50 ng/ml EGF or 10 ng/ml PDGF for 15 min and lysed in 1% Nonidet P-40 lysis buffer. Total cell lysates (40 μg) were separated by SDS/PAGE and transferred to PVDF membrane. Blots were analyzed using antibodies against pan-p85, p110α (BD Biosciences), pAKT (Cell Signaling), pS6K (Cell Signaling), pERK1/2 (Cell Signaling), β-actin (Cell Signaling).

ACKNOWLEDGMENTS. We thank Jeffrey Engelman for scientific advice, Roderick Bronson for histological analysis, and Carlos Garcia-Echeverria and Michel Maira (Novartis Institutes for Biomedical Research, Basel, Switzerland) for generously providing us with NVP-BEZ235. This work is supported by Dana Farber/Harvard Cancer Center Specialized Program Of Research Excellence grant 1P50CA127003-01 (to L.C.C., T.L.Y. and E.L.), and National Institutes of Health grants R37GM41890 (to L.C.C.), and R01-CA-115296 (to J.V.F.).

1. Samuels Y *et al* (2004) High frequency of mutations of the PIK3CA gene in human cancers. *Science* 304(5670):554.
2. Hennessy BT, Smith DL, Ram PT, Lu Y, Mills GB (2005) Exploiting the PI3K/AKT pathway for cancer drug discovery. *Nat Rev Drug Discov* 4(12):988–1004.
3. Carpten JD *et al* (2007) A transforming mutation in the pleckstrin homology domain of AKT1 in cancer. *Nature* 448(7152):439–444.
4. Huang CH *et al* (2007) The structure of a human p110alpha/p85alpha complex elucidates the effects of oncogenic PI3Kalpha mutations. *Science* 318(5857):1744–1748.
5. Miled N *et al* (2007) Mechanism of two classes of cancer mutations in the phosphoinositide 3-kinase catalytic subunit. *Science* 317(5835):239–242.
6. Isakoff SJ *et al* (2005) Breast cancer-associated PIK3CA mutations are oncogenic in mammary epithelial cells. *Cancer Res* 65(23):10992–11000.
7. Samuels Y *et al* (2005) Mutant PIK3CA promotes cell growth and invasion of human cancer cells. *Cancer Cell* 7(6):561–573.
8. Knight ZA, Shokat KM (2007) Chemically targeting the PI3K family. *Biochem Soc Trans* 35(Pt 2):245–249.
9. Ward SG, Finan P (2003) Isoform-specific phosphoinositide 3-kinase inhibitors as therapeutic agents. *Curr Opin Pharmacol* 3(4):426–434.
10. Folkman J (2007) Angiogenesis: An organizing principle for drug discovery? *Nat Rev Drug Discov* 6(4):273–286.
11. Fidler JJ (2003) The pathogenesis of cancer metastasis: The 'seed and soil' hypothesis revisited. *Nat Rev Cancer* 3(6):453–458.
12. Hofer E, Schweighofer B (2007) Signal transduction induced in endothelial cells by growth factor receptors involved in angiogenesis. *Thromb Haemost* 97(3):355–363.
13. Cantley LC (2002) The Phosphoinositide 3-Kinase Pathway. *Science* 296(5573):1655–1657.
14. Engelman JA *et al* (2005) ErbB-3 mediates phosphoinositide 3-kinase activity in gefitinib-sensitive non-small cell lung cancer cell lines. *Proc Natl Acad Sci USA* 102(10):3788–3793.
15. Engelman JA *et al* (2007) MET amplification leads to gefitinib resistance in lung cancer by activating ERBB3 signaling. *Science* 316(5827):1039–1043.
16. Chen J *et al* (2005) Akt1 regulates pathological angiogenesis, vascular maturation and permeability in vivo. *Nat Med* 11(11):1188–1196.
17. Phung TL *et al* (2006) Pathological angiogenesis is induced by sustained Akt signaling and inhibited by rapamycin. *Cancer Cell* 10(2):159–170.
18. Tothova Z *et al* (2007) FoxOs are critical mediators of hematopoietic stem cell resistance to physiologic oxidative stress. *Cell* 128(2):325–339.
19. Hamada K *et al* (2005) The PTEN/PI3K pathway governs normal vascular development and tumor angiogenesis. *Genes Dev* 19(17):2054–2065.
20. Johannessen CM *et al* (2008) TORC1 is essential for NF1-associated malignancies. *Curr Biol* 18(1):56–62.
21. Phung TL *et al* (2007) Endothelial Akt signaling is rate-limiting for rapamycin inhibition of mouse mammary tumor progression. *Cancer Res* 67(11):5070–5075.
22. Bader AG, Kang S, Vogt PK (2006) Cancer-specific mutations in PIK3CA are oncogenic in vivo. *Proc Natl Acad Sci USA* 103(5):1475–1479.
23. Ueki K *et al* (2002) Increased insulin sensitivity in mice lacking p85beta subunit of phosphoinositide 3-kinase. *Proc Natl Acad Sci USA* 99(1):419–424.
24. Luo J *et al* (2005) Class IA phosphoinositide 3-kinase regulates heart size and physiological cardiac hypertrophy. *Mol Cell Biol* 25(21):9491–9502.
25. Schlaeger TM (1997) Uniform vascular-endothelial-cell-specific gene expression in both embryonic and adult transgenic mice. *Proc Natl Acad Sci USA* 94(7):3058–3063.
26. Mao X, Fujiwara Y, Chapdelaine A, Yang H, Orkin SH (2001) Activation of EGFP expression by Cre-mediated excision in a new ROSA26 reporter mouse strain. *Blood* 97(1):324–326.
27. Yu J *et al* (1998) Regulation of the p85/p110 phosphatidylinositol 3′-kinase: Stabilization and inhibition of the p110alpha catalytic subunit by the p85 regulatory subunit. *Mol Cell Biol* 18(3):1379–1387.
28. Drake CJ, Fleming PA (2000) Vasculogenesis in the day 6.5 to 9.5 mouse embryo. *Blood* 95(5):1671–1679.
29. Jones EA, Baron MH, Fraser SE, Dickinson ME (2004) Measuring hemodynamic changes during mammalian development. *Am J Physiol Heart Circ Physiol* 287(4):H1561–9.
30. Brachmann SM *et al* (2005) Role of phosphoinositide 3-kinase regulatory isoforms in development and actin rearrangement. *Mol Cell Biol h* 25(7):2593–2606.
31. Furuyama T *et al* (2004) Abnormal angiogenesis in Foxo1 (Fkhr)-deficient mice. *J Biol Chem* 279(33):34741–34749.
32. Sun JF *et al* (2005) Microvascular patterning is controlled by fine-tuning the Akt signal. *Proc Natl Acad Sci USA* 102(1):128–133.
33. Schnell CR *et al* (2008) Effects of the dual pan-class I PI3K/mTOR inhibitor NVP-BEZ235 on the tumor vasculature: Implications for clinical imaging. *Manuscript under review.*
34. Jain RK (2005) Normalization of tumor vasculature: An emerging concept in antiangiogenic therapy. *Science* 307(5706):58–62.
35. Martin-Belmonte F, Mostov K (2008) Regulation of cell polarity during epithelial morphogenesis. *Curr Opin Cell Biol* 20(2):227–234.
36. Kölsch V, Charest PG, Firtel RA (2008) The regulation of cell motility and chemotaxis by phospholipid signaling. *J Cell Sci* 121(Pt 5):551–559.
37. Hoang MV, Senger DR (2005) In vivo and in vitro models of Mammalian angiogenesis. *Methods Mol Biol* 294:269–285.